https://doi.org/10.3311/PPch.42654

Periodica Polytechnica Chemical Engineering

Integrated Ozonation–Adsorption Pretreatment and Polyvinylidene Fluoride/Tungsten Based Polyoxometalate Photocatalytic Membrane for Produced Water Treatment

Tutuk Djoko Kusworo[1*], Adalia Veda[1], Rafi Mafazan[1], Hasrinah Hasbullah[2], Meitri Bella Puspa[1]

[1] Department of Chemical Engineering, Faculty of Engineering, Diponegoro University, 13 Jl. Prof. Soedarto, 50275 Semarang, Central Java, Indonesia
[2] Advanced Membrane Technology Research Center (AMTEC), School of Chemical & Energy Engineering (SCEE), Faculty of Engineering, Universiti Teknologi Malaysia, Block N29a, 81310 Skudai Johor, Malaysia
* Corresponding author, e-mail: tdkusworo@che.undip.ac.id

Received: 29 October 2025, Accepted: 19 January 2026, Published online: 13 February 2026

Abstract

The growing expansion of industrial operations, particularly within the oil and gas sector, has led to a substantial increase in produced water generation, an effluent rich in recalcitrant organic and inorganic contaminants. Conventional membrane based separations remain limited by low permeability and severe fouling, necessitating the development of more robust and multifunctional treatment systems. In this study, a durable photocatalytic hybrid membrane composed of polyvinylidene fluoride integrated with tungsten based polyoxometalate was fabricated *via* phase inversion. The incorporation of 2 wt% tungsten based polyoxometalate notably enhanced both permeability and contaminant rejection through improved interfacial compatibility and photocatalytic activity. Controlled ultraviolet irradiation for five minutes further optimized surface hydrophilicity and pore structure, achieving an outstanding water flux of 158.83 L/(m^2 h), while excessive exposure induced pore densification and reduced flux. A synergistic adsorption–ozonation pretreatment for three hours was integrated prior to photofiltration, resulting in 89% chemical oxygen demand removal and 85% ammonia nitrogen removal, effectively minimizing fouling and enhancing overall system stability. Under optimized conditions the membrane exhibited a steady permeate flux of 145 L/(m^2 h) over 600 minutes and achieved removal efficiencies of 99.0% chemical oxygen demand, 99.5% ammonia nitrogen, 20.5% total dissolved solids, and 6.87% phenol. These results demonstrate the combined effects of tungsten based polyoxometalate incorporation and pretreatment integration in improving both separation performance and operational durability. This work provides a scalable and sustainable strategy toward next-generation hybrid photocatalytic membranes for advanced produced water purification.

Keywords

photocatalytic membrane, polyoxometalate, ozonation–adsorption, produced water

1 Introduction

Produced water (PW), a major byproduct of oil and gas extraction processes represents one of the most pressing environmental challenges due to its substantial volume and chemically diverse nature [1]. Each barrel of oil produced can generate several barrels of PW, which often contains dispersed hydrocarbons [2], dissolved organics, metal ions, sulfides, and high salinity components [3–5]. The coexistence of these contaminants, coupled with suspended particulates and residual chemical additives, renders PW an exceptionally difficult waste matrix to treat and reuse effectively. Conventional treatment strategies such as coagulation–flocculation [6], gravity separation [7], or biological degradation [8] have been widely applied. However, these conventional approaches frequently exhibit limited efficiency in eliminating persistent and hazardous contaminants. Furthermore, their poor adaptability to the variable composition of produced water, coupled with the tightening environmental discharge regulations, underscores the necessity for more advanced, integrated, and sustainable treatment technologies.

Among advanced oxidation processes (AOPs), ozonation has emerged as a promising approach for decomposing refractory organic pollutants into smaller and more biodegradable intermediates [9]. This process depends on

Cite this article as: Kusworo, T. D., Veda, A., Mafazan, R., Hasbullah, H., Bella Puspa, M. "Integrated Ozonation–Adsorption Pretreatment and Polyvinylidene Fluoride/Tungsten Based Polyoxometalate Photocatalytic Membrane for Produced Water Treatment", Periodica Polytechnica Chemical Engineering, 2026. https://doi.org/10.3311/PPch.42654

the *in situ* generation of hydroxyl radicals (•OH), which are powerful, non-selective oxidants capable of mineralizing a wide range of contaminants. Nevertheless, the practical application of ozonation as a standalone technique is constrained by intrinsic drawbacks such as the short lifetime of reactive radicals, poor ozone solubility and mass transfer in aqueous systems, and substantial energy requirements [10, 11]. As a result, incomplete oxidation and the formation of secondary by-products often occur. To address these limitations, coupling ozonation with adsorption pretreatment has gained significant attention [12]. Adsorption, utilizing porous materials such as bentonite, activated carbon or zeolite, can effectively remove hydrophobic and ionic pollutants, thereby reducing the organic load prior to ozonation and enhancing the utilization efficiency of ozone. This combined ozonation–adsorption process offers a synergistic mechanism that not only enhances degradation kinetics and pollutant removal but also minimizes catalyst deactivation and downstream fouling [13].

In parallel with pretreatment advancements membrane photocatalysis has emerged as a highly effective technology capable of integrating pollutant separation and degradation within a single operational system. Photocatalytic membranes merge the physical selectivity of membrane filtration with the oxidative degradation capability of photocatalysis, enabling continuous operation with minimal secondary contamination [14, 15]. In the context of produced water treatment, ultrafiltration membranes are particularly suitable due to their ability to retain macromolecular organic matter, colloids, and oil-associated aggregates while maintaining relatively high permeate flux. Among available polymeric substrates, poly(vinylidene fluoride) (PVDF) is widely recognized for its excellent thermal resistance, chemical inertness, and mechanical robustness, making it one of the most commonly employed materials for ultrafiltration membrane fabrication *via* non-solvent induced phase separation [16]. However, pristine PVDF is inherently hydrophobic and lacks photocatalytic functionality, necessitating surface or structural modification to enable reactive separations [17]. Incorporating polyoxometalate (POM) compounds, particularly tungsten based POM, into PVDF matrices has proven to be a powerful modification route. POM are discrete, nanoscale metal–oxygen clusters characterized by high redox flexibility, reversible electron transfer, and structural stability. When embedded into a PVDF ultrafiltration membrane framework, tungsten based POMs serve as photoactive centers that enhance light absorption, promote charge separation, and improve hydrophilicity and antifouling characteristics [18, 19].

Despite these advances, standalone photocatalytic membranes often face challenges in treating the highly variable and complex chemical matrix of produced water. Organic macromolecule fouling, potential leaching of active species, and the incomplete degradation of persistent contaminants can restrict the long-term stability and scalability of such systems. To address these limitations, the present study adopts a hybrid treatment strategy combining adsorption–ozonation pretreatment with a PVDF based ultrafiltration photocatalytic membrane. The pretreatment stage effectively breaks down and captures large organic molecules, mitigating fouling, while the subsequent PVDF/W based POM photocatalytic membrane further mineralizes residual pollutants under light irradiation. This hybrid configuration provides a multi-barrier system that leverages physical adsorption, chemical oxidation, and photocatalytic degradation synergistically, resulting in enhanced purification performance, operational durability, and overall energy efficiency.

2 Materials and methods

2.1 Materials

The membrane fabrication process utilized PVDF (SOLEF 6020/1001, 99%) with number average molar mass M_n = 153 g/mol, weight average molar mass M_w = 352 g/mol as the base polymer, which was acquired from Sigma-Aldrich Chemie (Germany). N-Methyl-2-pyrrolidone (NMP, 85%), supplied by Merck, served as the solvent in the dope preparation, while deionized water sourced from Indrasari, Semarang, acted as the coagulation medium. Zeolite was incorporated as an adsorptive component in the pretreatment step to enhance contaminant removal. The synthesis and modification procedures employed analytical-grade reagents, namely potassium permanganate, nitric acid, sodium tungstate dihydrate ($Na_2WO_4 \cdot 2H_2O$), terephthalic acid (H_2BDC), N,N-dimethylformamide (DMF), and tungsten trioxide (WO_3), all obtained from Merck.

2.2 Fabrication of polyvinylidene fluoride/tungsten based polyoxometalate-membrane

The synthesis of PVDF/W based POM membranes was conducted through a controlled phase inversion method to ensure the uniform dispersion of photocatalytic nanoparticles within the polymer matrix. Initially, 2 wt% W based POM nanoparticles were dispersed in NMP *via* ultrasonic agitation for 60 min to achieve a stable colloidal

suspension. Subsequently, PVDF (13 wt%) was gradually introduced into the nanoparticle suspension and continuously stirred at 60–70 °C for approximately 10 h until a clear and homogeneous casting solution was obtained. The resulting solution was then left undisturbed at room temperature for 24 h to facilitate degassing and the removal of entrapped air bubbles. Membrane films were prepared by casting the polymer solution onto a clean glass substrate using a 150 μm casting knife, followed by brief UV exposure to enhance interfacial bonding and photocatalyst stability. The cast films were immersed in deionized water for 24 h to induce phase separation, and the resulting membranes were subsequently dried at 30 °C for 24 h to yield flexible and defect-free structures.

2.3 Characterization of polyvinylidene fluoride/tungsten based polyoxometalate membrane

The surface morphology of the prepared membranes was examined using a field-emission scanning electron microscope (FE-SEM, JEOL JSM-6510LA, Japan) to assess their structural uniformity and pore architecture. The chemical functionalities and potential bonding interactions among the membrane components were investigated using Fourier transform infrared (FTIR) spectroscopy (Thermo Fischer Scientific RaptIR, USA), offering valuable information on the modifications in surface chemistry resulting from POM incorporation. Furthermore, the nanoscale topography and roughness characteristics were analyzed through atomic force microscopy (AFM, Park NX10, USA) operated in tapping mode, enabling high-resolution visualization of the membrane surface features.

2.4 Membrane performance evaluation

The performance of the fabricated membranes was assessed through photofiltration experiments using produced water as the feed solution. All filtration tests were conducted in a continuous cross-flow filtration mode to minimize concentration polarization and fouling effects. The experiments were performed at a constant transmembrane pressure of 5 bar, an operating temperature of 25 ± 2 °C, and an active membrane area of $1.26 \cdot 10^{-3}$ m^2. The recovery was defined as the ratio of permeate flow rate to feed flow rate and was maintained at a constant value throughout the experiments. Evaluation parameters included permeate flux and the removal efficiencies of chemical oxygen demand, phenol, and ammonia nitrogen. Prior to testing, each membrane was compacted with deionized water at 5 bar for 30 min to ensure hydraulic stability. Subsequent filtration was conducted at 5 bar with an active membrane area of $1.26 \cdot 10^{-3}$ m^2. Permeate was collected at 30 min intervals, and the water flux was determined according to Eq. (1):

$$J = \frac{\Delta V}{S \cdot \Delta t}, \tag{1}$$

where J denotes the permeate flux ($L/(\text{m}^2\,\text{h})$), where ΔV is the permeate volume (L) collected over the filtration time Δt (h), and S is the effective membrane area (m^2).

The concentrations of chemical oxygen demand, phenol, and ammonia nitrogen in both feed and permeate samples were measured using a Thermo Scientific Genesys 10s UV–Vis spectrophotometer (Thermo Electron Scientific Instruments LLC., Madison, WI, USA). The rejection efficiencies were subsequently calculated using Eq. (2):

$$R_E = \left(1 - \frac{C_t}{C_o}\right) \cdot 100\%, \tag{2}$$

where R_E is the pollutant removal efficiency (%), C_t and C_o are the contaminant concentrations in the permeate and feed, respectively.

2.5 Pretreatment process

The pretreatment sequence was designed as a coupled adsorption–ozonation process to enhance contaminant degradation prior to membrane photofiltration. In the adsorption stage, produced water was continuously passed through a fixed-bed column packed with commercial zeolite, facilitating the removal of hydrophobic organics and ammoniacal species through ion exchange and surface adsorption mechanisms. The contact time was maintained for 1–3 h, during which effluent samples were periodically collected at 30 min intervals to quantify reductions in COD, NH_3–N, and phenolic compounds. Upon achieving approximately 1 L of adsorbate-treated effluent, the stream was subsequently subjected to ozonation using a laboratory-scale unit (Aquazon JQ0518, China) operated at a constant ozone dosage of 70 mg/L and a flow rate of 0.5 L/min. The ozonation process, sustained for 1–3 h. The pretreated effluent was then directed to the photocatalytic membrane module for final purification under controlled photofiltration conditions.

2.6 Stability of polyvinylidene fluoride/tungsten based polyoxometalate membranes

Prior to conducting the stability test, each membrane sample was pre-conditioned by flushing with deionized water

under a transmembrane pressure of 5 bar for 30 min to achieve steady-state permeability and remove any residual impurities. The long-term operational stability was subsequently assessed through continuous photofiltration using produced water as the feed solution. The experiments were carried out under a constant transmembrane pressure of 5 bar, at ambient temperature (25 ± 2 °C), and with an effective membrane surface area of $1.26 \cdot 10^{-3}$ m^2. The photofiltration process was maintained for a total duration of 600 min. Permeate samples were collected and analyzed separately at 30 min intervals, rather than being combined, to monitor the temporal stability of membrane performance over the entire operation period. The stability of the PVDF/W based POM membranes was evaluated by quantifying the levels of COD, NH_3–N, phenol, and TDS in the collected permeates.

3 Results and discussion

3.1 Produced water characteristics

Produced water is an inevitable effluent generated during oil extraction activities and is characterized by a complex mixture of organic pollutants, inorganic salts, suspended solids, and residual hydrocarbons. Its chemical profile is highly variable and strongly influenced by multiple factors, including the geographic setting, reservoir geology, formation water chemistry, and the operational practices applied during drilling and production. Owing to this variability, site-specific characterization of produced water is essential to accurately assess its environmental impact and to design effective treatment strategies. This issue is particularly relevant in Indonesia, where extensive oil exploration and production activities necessitate careful evaluation of produced water prior to disposal or reuse. In the present study, the analyzed produced water exhibited contaminant concentrations that exceeded the permissible limits specified by both national and international environmental regulations [20]. According to Indonesia's Ministerial Regulation No. 19 of 2010 [21], wastewater discharged from oil, gas, and geothermal operations must comply with maximum allowable concentrations of 4000 mg/L for total dissolved solids (TDS), 200 mg/L for chemical oxygen demand (COD), 25 mg/L for total oil and grease, and 5 mg/L for NH_3–N. However, the measured values particularly for COD and NH_3–N were substantially higher than these regulatory thresholds, confirming the inadequacy of untreated produced water for direct discharge. These substances are often released from subsurface formations or mobilized during fluid mixing processes, further complicating the treatment of produced water and underscoring the need for advanced purification technologies. The detailed physicochemical composition of the produced water used as feed for membrane testing is summarized in Table 1 [22–26].

3.2 SEM surface analysis

The surface morphology of the fabricated membranes was examined using SEM. The neat PVDF membrane (Fig. 1 (a)) exhibits a relatively smooth and homogeneous surface structure with uniformly distributed pores. These surface pores, which are characteristic of PVDF membranes fabricated via phase inversion, facilitate permeate transport but also indicate limited surface roughness. The overall smoothness of the PVDF neat surface suggests the dominance of the dense skin layer formation during solvent–nonsolvent exchange, which is typical for pure polymeric membranes without inorganic fillers. In contrast, the PVDF/W based POM membrane (Fig. 1 (b)) displays a more heterogeneous and textured surface morphology, attributed to the incorporation of W based POM nanoparticles within the polymer matrix. The embedded bright spots observed on the membrane surface correspond to the presence of dispersed POM domains, confirming successful integration of the photocatalytic component. The local aggregation of W based POM particles likely enhances the interfacial roughness and alters the microstructural topology of the surface. This morphological

Table 1 The properties of contaminants in the sample of produced water obtained from oil and gas production in Cirebon, Indonesia

Parameters	Value	Method	Local standards	International standards	Unit
pH	7.34 ± 0.015	pH meter	6–9	6.5–8.5	–
TDS	4629 ± 0.58	TDS meter	4000	1200	mg/L
Total suspended solids (TSS)	136 ± 0.28	SNI 06-6989.25-2005 [22]	–	30	mg/L
COD	1000 ± 1.36	SNI 6989.2:2019 [23]	200-300	<50	mg/L
Biochemical oxygen demand (BOD)	310 ± 0.88	SNI 6989.72:2009 [24]	80	<30	mg/L
Total oils and fats	15 ± 1.51	SNI 6989.10:2011 [25]	25–50	–	mg/L
NH_3–N	665.54 ± 1.05	SNI 06-6989.30-2005 [26]	5	100	mg/L

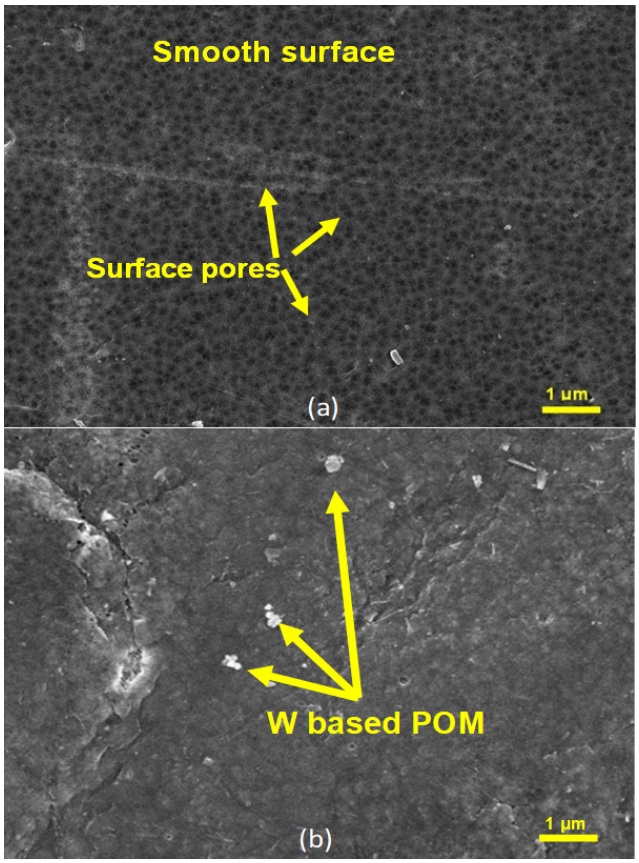

Fig. 1 SEM surface morphology (a) PVDF neat and (b) PVDF/W based POM membranes

transformation may facilitate improved hydrophilicity and interfacial charge transfer during photocatalytic operation. The pronounced surface roughness exhibited by the composite membrane may be attributed to the accelerated phase separation kinetics occurring during the casting process, which are likely governed by interfacial interactions between the dispersed nanoparticles and the polymer matrix [27]. These morphological alterations are particularly advantageous for photocatalytic membrane systems, as they facilitate an increased density of catalytically active sites, promote enhanced photon scattering within the membrane matrix, and improve interfacial interactions between the membrane surface and pollutant molecules present in the feed solution [28]. These features collectively contribute to the superior permeation and photocatalytic performance observed in the PVDF/W based POM membranes compared with the PVDF neat.

3.3 Surface roughness

AFM analysis was conducted to quantitatively evaluate the influence of W based POM incorporation on the surface morphology of the PVDF membranes, as illustrated in Fig. 2. The PVDF neat membrane (Fig. 2 (a)) exhibited a relatively smooth and uniform topography characterized by shallow surface undulations, indicating the dense and homogeneous structure typical of membranes formed through non-solvent induced phase separation (NIPS). In contrast, the PVDF/W based POM membrane (Fig. 2 (b)) demonstrated a significantly rougher and more irregular surface profile, with distinct elevations and depressions distributed across the membrane plane. The quantitative roughness parameters derived from AFM measurements reveal a notable enhancement in surface textural features following POM incorporation. The average roughness (R_a) increased from 8.3 nm for PVDF neat to 28.1 nm for PVDF/W based POM, while the root mean square roughness (R_q) rose from 10.7 nm to 45.4 nm confirming a more heterogeneous and microstructured surface. These changes suggest that the embedded W based POM nanoparticles acted as nucleation sites during phase inversion, interrupting polymer chain packing and inducing microscale surface corrugation [29].

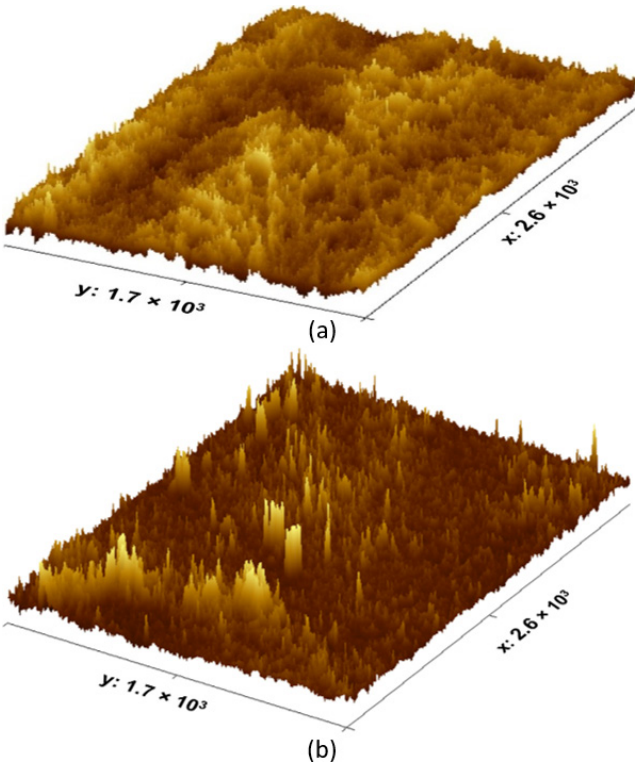

Fig. 2 Surface roughness of (a) PVDF neat and (b) PVDF–W-based POM membranes (the unit corresponding to the axes values is µm)

Although AFM does not directly determine membrane pore size, the nanometer-scale surface roughness and dense top-layer morphology observed are characteristic of polyvinylidene fluoride ultrafiltration membranes fabricated *via* non-solvent induced phase separation. Such modification in the surface topology is beneficial for membrane–liquid interactions. The increased surface roughness contributes

to a larger effective contact area, promoting enhanced hydrophilicity and water permeability. The intrinsic hydrophilicity and high surface energy of W based POM clusters facilitate more effective water molecule adsorption and spreading, counteracting the hydrophobic nature of the PVDF backbone [30]. Consequently, the improved wettability reduces interfacial resistance to water transport, resulting in higher initial flux and enhanced long-term permeation stability. The formation of micro/nano-scale roughness enhances the light-scattering capability of the membrane surface, which can improve photon absorption efficiency during photocatalytic operation. This morphological characteristic allows more active sites to be exposed and increases the likelihood of charge transfer at the membrane–solution interface. Nevertheless, excessive roughness may potentially aggravate fouling by promoting the physical entrapment of organic matter within surface asperities. Therefore, the moderate roughness observed in PVDF–W based POM membranes represents an optimal compromise between increased hydrophilicity, photocatalytic efficiency, and antifouling resistance.

3.4 FTIR analysis

The FTIR spectra provide profound insight into the molecular-level interactions and structural transformations occurring within the PVDF matrix upon the incorporation of W based POM as presented in Fig. 3. For the PVDF neat membrane, the spectral signatures are dominated by vibrational modes characteristic of the α-crystalline phase, reflecting its semi-crystalline fluoropolymer nature. The absorption bands observed at 1400–1450 cm^{-1} correspond to CH_2 bending vibrations, whereas the peaks within 1175–1250 cm^{-1} are assigned to symmetric and asymmetric stretching of CF_2 groups, confirming the dominance of the non-polar α-phase configuration [31]. The prominent absorption at approximately 840–880 cm^{-1} is attributed to the C–F stretching vibrations of PVDF chains, while a weak band near 1650 cm^{-1} may be ascribed to residual C=C stretching, likely arising from unsaturated end groups or polymerization by-products. These spectral characteristics collectively confirm the highly ordered chain conformation of the PVDF neat structure. The incorporation of W based POM into the PVDF matrix, substantial modifications in spectral features are evident, signifying the occurrence of strong physicochemical interactions at the polymer–inorganic interface. The noticeable attenuation of CF_2 and C–F band intensities indicates a perturbation of the α-phase crystalline domains, implying either a partial α to β phase transition or an increase in amorphous content. The β-phase of PVDF, characterized by an all-trans (TTT) chain conformation, is known to exhibit higher dipole orientation and enhanced electroactivity, which could significantly improve interfacial charge separation in photocatalytic applications [32]. The observed modification in the crystalline phase composition thus suggests that the presence of POM clusters induces local electric field heterogeneity, acting as a polarizing agent that promotes β-phase nucleation.

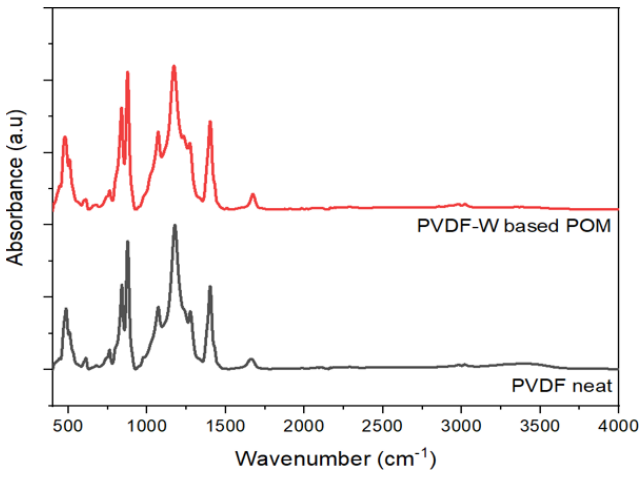

Fig. 3 FTIR analysis

The broadening and intensification of absorption features in the 2800–3000 cm^{-1} region corresponding to C–H stretching vibrations reflect the establishment of weak hydrogen bonding and dipole–dipole interactions between the PVDF backbone and the oxygen-rich POM surface [33]. These interactions are indicative of improved compatibility and interfacial adhesion, which play a crucial role in suppressing nanoparticle agglomeration and facilitating homogeneous dispersion of the inorganic phase within the polymer matrix. In addition, the appearance of new vibrational bands in the 500–700 cm^{-1} region can be unequivocally attributed to metal–oxygen (W–O) stretching modes, confirming the successful immobilization and structural integrity of the W based POM entities within the hybrid membrane framework. Collectively, these FTIR findings elucidate the intricate interfacial chemistry governing the PVDF/W based POM nanocomposite system. This synergistic interfacial structure is expected to facilitate efficient charge carrier migration, enhance dipole polarization under illumination, and ultimately improve the photocatalytic response and operational stability of the membrane during produced water treatment.

3.5 Effect of UV light on membrane performance

As depicted in Fig. 4, the PVDF/W based POM membranes exposed to ultraviolet irradiation for 5 min demonstrated the most stable and efficient. The membranes achieved an initial water flux of approximately

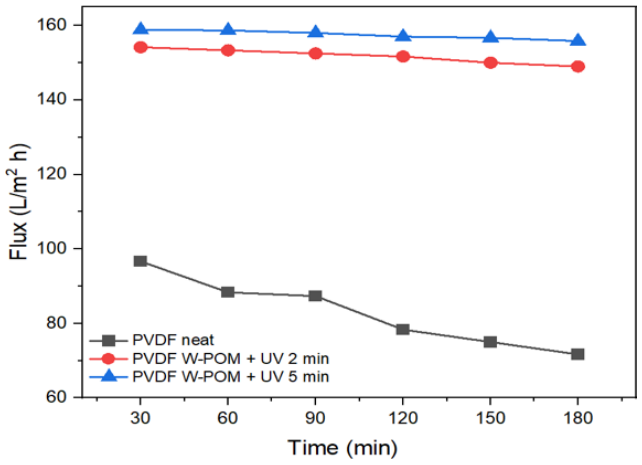

(a)

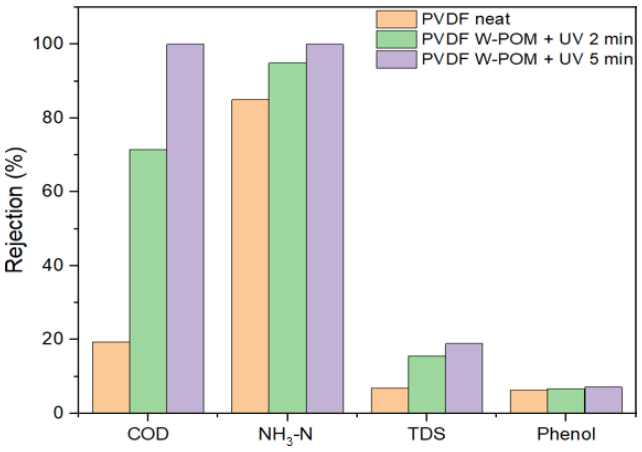

(b)

Fig. 4 Flux (a) and rejection performance (b) of PVDF neat and PVDF/W-based POM membranes under ultraviolet irradiation at a transmembrane pressure of 5 bar

158.83 L/(m² h) within the first 30 min of operation, with only a marginal decline to 155.83 L/(m² h) during the final 30 min, indicating excellent hydraulic stability and structural integrity under continuous filtration conditions. In contrast, the PVDF neat membranes exposed to UV (Neat + UV) demonstrated markedly lower permeate flux, decreasing from 96.67 L/(m² h) to 71.67 L/(m² h) over the same period. These findings underscore the positive influence of controlled UV irradiation on membranes permeability, particularly in enhancing water transport dynamics. The observed improvement in flux is closely associated with the increased surface hydrophilicity induced by UV exposure. Ultraviolet radiation initiates surface photochemical transformations, leading to the incorporation of polar functional groups such as hydroxyl (–OH) and carbonyl (C=O) into the polymeric matrix. These moieties increase the surface energy and affinity for water molecules, thereby reducing interfacial resistance and facilitating more efficient permeation [34, 35]. Additionally, UV exposure can cause localized polymer chain scission or surface restructuring, which may contribute to the enlargement of pore structures and an overall increase in membranes porosity. The extent of hydrophilic enhancement is also influenced by the density of grafted monomers on the membranes surface. As the concentration of hydrophilic moieties increases, a more compact and uniform graft layer is formed, thereby improving water sorption and flux. The incorporation of photoresponsive inorganic nanomaterials further enhances this effect by introducing photocatalytic functionality and improving the membranes's resistance to UV-induced degradation [36]. These nanostructures act as radical scavengers, mitigating polymer breakdown while concurrently facilitating the oxidative degradation of organic pollutants during operation [37]. However, it is crucial to regulate the UV irradiation duration, as excessive exposure (>5 min) has been shown to produce adverse effects. Prolonged UV treatment intensifies photo-crosslinking and accelerates the formation of a highly compact selective layer, which restricts pore connectivity and significantly diminishes flux [38]. Moreover, extended irradiation induces alterations in the polymer's thermal behavior and phase transition properties, consistent with oxidative degradation, polymer recombination, and morphological densification processes. These phenomena ultimately reduce membranes permeability and operational efficiency. UV-modified membranes demonstrated enhanced rejection of TDS and COD relative to unmodified membranes. The denser membranes layer formed via photochemical crosslinking impedes solute passage, thereby improving contaminant retention [39].

Simultaneously, UV irradiation contributes to the photodecomposition of complex organic molecules into simpler and smaller compounds, further supporting the observed reduction in COD and TDS concentrations.

3.6 Effect of pretreatment on the performance of the membranes

Pretreatment plays a critical role in wastewater treatment systems by reducing pollutant concentrations before membranes filtration. This process helps to minimize membranes fouling, enhance overall system efficiency, and extend membranes lifespan. In this study, the individual and synergistic effects of ozonation and adsorption pretreatments were investigated to evaluate their contributions to membranes separation performance. As presented

in Fig. 5, longer pretreatment durations particularly 3 h treatments yielded significantly higher pollutant rejection compared to shorter treatments (1 h). Ozonation achieved removal efficiencies of 89% for COD and 85% for NH_3–N, while TDS and phenol removal reached 12.61% and 4%, respectively. Similarly, adsorption pretreatment resulted in 85%, 80%, 13%, and 3.5% removal of COD, NH_3–N, TDS, and phenol respectively. Ozonation, an AOPs facilitates the degradation of complex organic pollutants through the generation of highly reactive hydroxyl radicals (•OH). Upon dissolution in water, ozone decomposes to form reactive species capable of breaking down large, hydrophobic molecules such as hydrophilic fragments *via* mineralization [40]. This process is vital for minimizing membranes fouling and improving permeate flux, as evidenced by the PVDF/W based POM membranes treated with 3 h ozonation, which exhibited the highest flux values due to enhanced organic degradation. A key advantage of ozonation is its ability to operate without generating secondary sludge, thereby simplifying downstream treatment and supporting sustainable wastewater management [41]. Additionally, it promotes the transformation of natural organic matter (NOM) into more biodegradable compounds, reducing the pollutant load and contributing to stable membranes operation [42]. In parallel, adsorption using zeolite based materials has gained attention for its simplicity, cost-effectiveness, and favorable performance under mild conditions. Zeolites, comprising a crystalline framework of aluminosilicate units, provide a high surface area and excellent ion-exchange capacity. Chemical activation increases the number of exchangeable H^+ ions, thereby enhancing adsorption efficiency [43]. However, excessive acid treatment can compromise the pore structure, reducing adsorption performance. In this study, adsorption effectively removed recalcitrant organic compounds and improved overall membranes rejection, especially when integrated with ozonation [44]. The sequential application of adsorption followed by ozonation was found to be particularly effective. Adsorption preferentially captures high-molecular-weight organics, allowing ozonation to subsequently degrade the remaining low-molecular-weight compounds. This approach accelerates degradation kinetics, reduces membranes fouling, and promotes flux stability and membranes durability [45]. The improvement is attributed to the extended ozone residence time, which enhances the generation of hydroxyl radicals and increases the extent of pollutant oxidation. Membranes subjected to the combined pretreatment showed significantly higher rejection of COD, TDS,

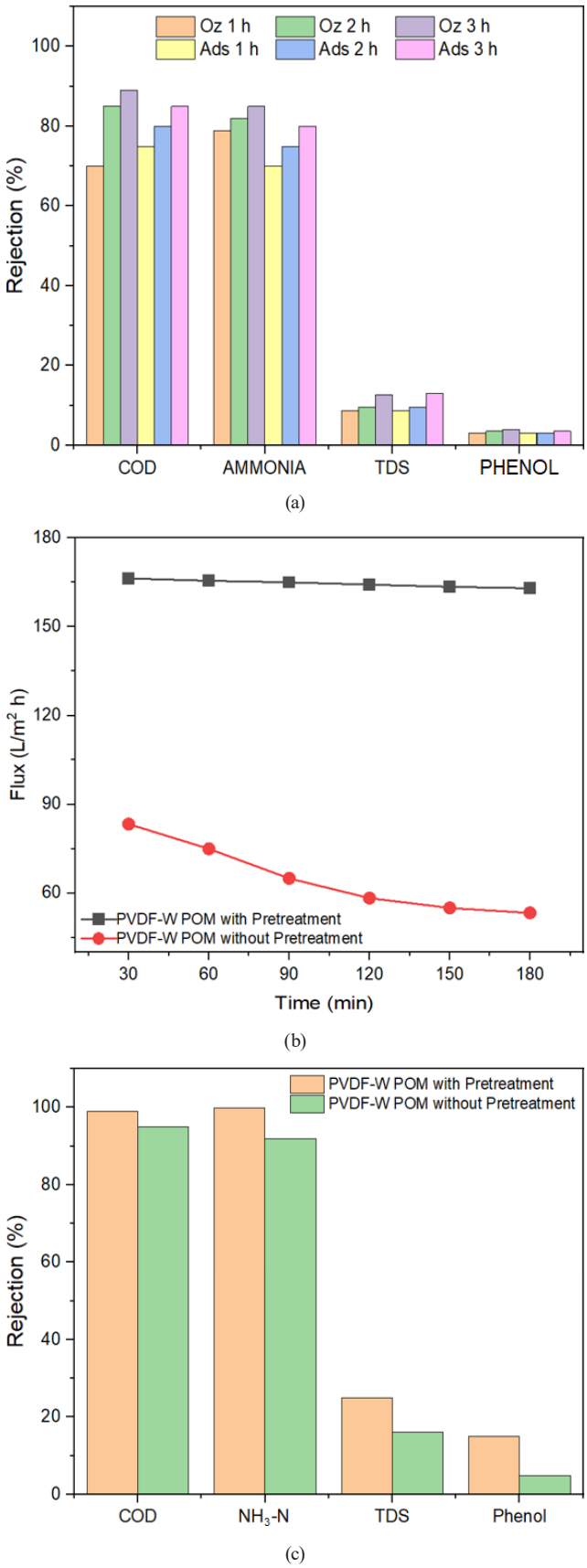

Fig. 5 Adsorption–ozonation pretreatment (a) flux behavior (b), and rejection efficiency (c) of membranes coupled with the pretreatment process

NH_3–N, and phenol. This enhanced performance is associated with increased oxidative degradation resulting from prolonged ozonation, which elevates hydroxyl radical concentrations and accelerates contaminant breakdown. Furthermore, surface adsorption is known to facilitate photocatalytic degradation by increasing the contact frequency between active sites and pollutants, thus enhancing removal efficiency, particularly in systems employing photoactive materials. In conclusion, the integrated pretreatment strategy involving 3 h ozonation and 3 h adsorption offers an effective, scalable, and environmentally friendly solution for treating complex effluents such as produced water. This dual-stage approach maximizes pollutant rejection, improves flux stability, and significantly enhances the overall performance of membranes filtration systems in advanced water treatment applications.

3.7 Membrane stability

The stability and rejection performance of the membranes were evaluated using produced water as the feed solution. The flux decline profiles clearly indicate that the PVDF-W-based POM membrane exhibited significantly better flux stability compared to the neat PVDF membrane, as shown in Fig. 6. PVDF/W based POM showed a high permeate flux of approximately 145 L/(m^2 h) which gradually decreased to around 117 L/(m^2 h) after 600 min filtration, corresponding to about 80.7% flux retention. In comparison, the PVDF neat membrane exhibited a substantially lower initial permeate flux of approximately 37 L/(m^2 h) which progressively decreased to nearly 10 L/(m^2 h) over the course of operation, corresponding to a flux retention of only about 27% of its initial value. This marked difference suggests that W based POM incorporation effectively improves the membrane's resistance to fouling and maintains permeability over prolonged operation.

Regarding rejection performance, PVDF/W based POM demonstrated substantially higher removal efficiencies for key contaminants present in produced water compared to PVDF neat. COD rejection increased drastically from 5.83% for PVDF neat to complete removal (99%) for PVDF–W based POM. Similarly, NH_3–N rejection improved from 63.66% to 99.5%, TDS from 2.17% to 20.5%, and phenol rejection increased modestly from 3.81% to 6.87%. These results indicate that the W based POM modified membrane not only maintains higher flux but also enhances selective separation of pollutants commonly found in produced water. The improved performance

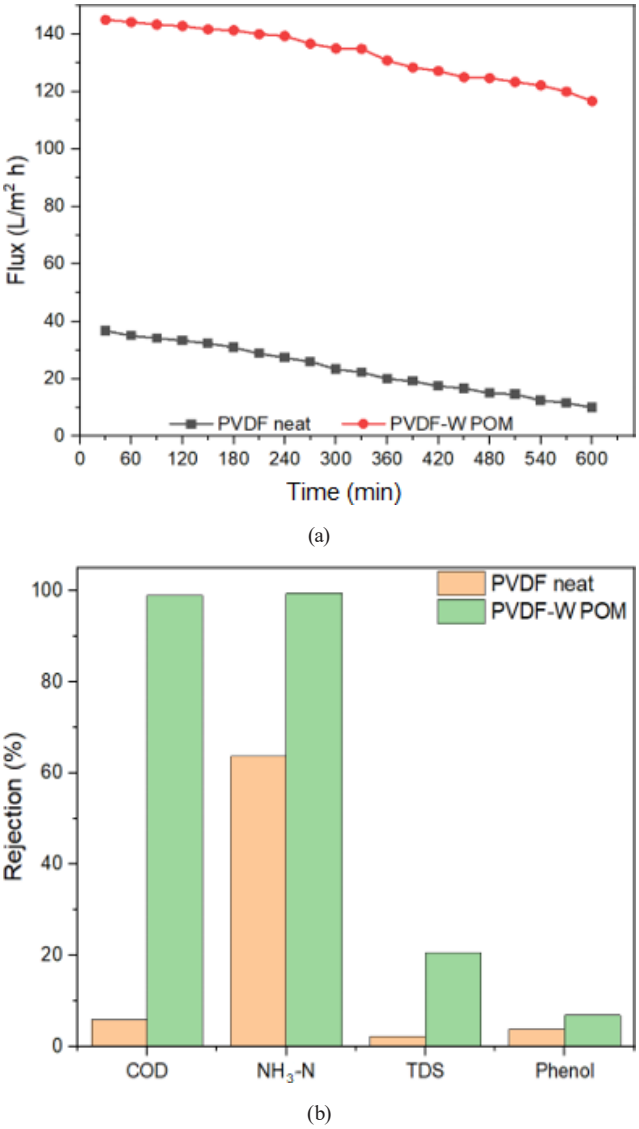

(a)

(b)

Fig. 6 The result of reusability test (a) and pollutant rejection (b)

of W based POM can be attributed to the unique structural and chemical properties introduced by the W based POM. The nanoparticle provides additional porous pathways and increases membrane hydrophilicity, which facilitates water permeation while reducing the accumulation of foulants on the membrane surface. The high surface area and tunable pore size of W based POM also contribute to the effective adsorption and size exclusion of organic and inorganic contaminants, thus enhancing rejection. In contrast, the neat PVDF membrane lacks these features, making it more susceptible to fouling and pore blockage, which leads to rapid flux decline and poor contaminant removal. Overall, these findings demonstrate that the incorporation of W based POM into PVDF membranes significantly improves their applicability for produced water treatment by enhancing both operational stability and treatment

efficiency. This modification addresses critical challenges in oilfield wastewater management, enabling longer membrane lifespan and more effective removal of complex pollutants such as organics, NH_3–N, and dissolved solids.

4 Conclusion

This study successfully developed a robust and multifunctional PVDF/W based POM photocatalytic membrane integrated with an adsorption–ozonation pretreatment system for efficient produced water treatment. The incorporation of 2 wt% W based POM significantly enhanced membrane permeability and pollutant rejection through improved interfacial bonding and photocatalytic activity. UV irradiation (5 min) further optimized membrane surface energy and pore morphology, yielding a superior flux of 158.83 L/(m^2 h) with excellent hydraulic stability. The integrated adsorption–ozonation pretreatment achieved up to 89% COD and 85% NH_3–N removal, effectively mitigating fouling and improving long-term performance. Under continuous operation for 600 min, the optimized membrane maintained a stable flux of 145 L/(m^2 h) and achieved exceptional removal efficiencies of 99% COD, 99.5% NH_3–N, 20.5% TDS, and 6.87% phenol. This approach provides valuable insights for scaling up hybrid photocatalytic membranes capable of addressing the challenges of complex industrial wastewater, particularly in the oil and gas sector, while promoting environmentally responsible water management.

Acknowledgements

This project is financially supported by the grant of Publication Acceleration Research Diponegoro (RAP UNDIP) No. 222-237/UN7.D2/PP/IV/2025. Special gratitude to the Institute for Research and Community Services, Diponegoro University (LPPM UNDIP) for the assistance during the completion of this project.

References

[1] Beyer, J., Goksøyr, A., Hjermann, D. Ø., Klungsøyr, J. "Environmental effects of offshore produced water discharges: A review focused on the Norwegian continental shelf", Marine Environmental Research, 162, 105155, 2020. https://doi.org/10.1016/j.marenvres.2020.105155

[2] Vijayanand, M., Ramakrishnan, A., Subramanian, R., Issac, P. K., Nasr, M., …, Ravindran, B. "Polyaromatic hydrocarbons (PAHs) in the water environment: A review on toxicity, microbial biodegradation, systematic biological advancements, and environmental fate", Environmental Research, 227, 115716, 2023. https://doi.org/10.1016/j.envres.2023.115716

[3] Farnan, J., Vanden Heuvel, J. P., Dorman, F. L., Warner, N. R., Burgos, W. D. "Toxicity and chemical composition of commercial road palliatives versus oil and gas produced waters", Environmental Pollution, 334, 122184, 2023. https://doi.org/10.1016/j.envpol.2023.122184

[4] Amakiri, K. T., Ogolo, N. A., Angelis-Dimakis, A., Albert, O. "Physicochemical assessment and treatment of produced water: A case study in Niger delta Nigeria", Petroleum Research, 8(1), pp. 87–95, 2023. https://doi.org/10.1016/j.ptlrs.2022.05.003

[5] Tan, B., He, Z., Fang, Y., Zhu, L. "Removal of organic pollutants in shale gas fracturing flowback and produced water: A review", Science of The Total Environment, 883, 163478, 2023. https://doi.org/10.1016/j.scitotenv.2023.163478

[6] Li, J., How, Z. T., Benally, C., Sun, Y., Zeng, H., Gamal El-Din, M. "Removal of colloidal impurities by thermal softening-coagulation-flocculation-sedimentation in steam assisted gravity drainage (SAGD) produced water: Performance, interaction effects and mechanism study", Separation and Purification Technology, 313, 123484, 2023. https://doi.org/10.1016/j.seppur.2023.123484

[7] Chen, L., Zhou, J., Li, K., Wu, X., Chen, Z., …, Wu, W. "Robust and stable organic sulfonate sodium salt-coated superhydrophilic mesh for ultra-fast gravity-drive oil-water separation", Surfaces and Interfaces, 49, 104331, 2024. https://doi.org/10.1016/j.surfin.2024.104331

[8] Freedman, D. E., Riley, S. M., Jones, Z. L., Rosenblum, J. S., Sharp, J. O., Spear, J. R., Cath, T. Y. "Biologically active filtration for fracturing flowback and produced water treatment", Journal of Water Process Engineering, 18, pp. 29–40, 2017. https://doi.org/10.1016/j.jwpe.2017.05.008

[9] Kusworo, T. D., Puspa, M. B., Kumoro, A. C., Sutapa, I. D. A., Dalanta, F., Utomo, D. P. "Manufacture and performance assessment of PVDF-La@TiO_2 Photocatalyst implanted membrane for efficient produced water treatment via ozonation-adsorption process under visible-light exposure", Journal of Water Process Engineering, 67, 106179, 2024. https://doi.org/10.1016/j.jwpe.2024.106179

[10] Lim, S., Shi, J. L., von Gunten, U., McCurry, D. L. "Ozonation of organic compounds in water and wastewater: A critical review", Water Research, 213, 118053, 2022. https://doi.org/10.1016/j.watres.2022.118053

[11] Das, P. P., Dhara, S., Samanta, N. S., Purkait, M. K. "Advancements on ozonation process for wastewater treatment: A comprehensive review", Chemical Engineering and Processing - Process Intensification, 202, 109852, 2024. https://doi.org/10.1016/j.cep.2024.109852

[12] Aryanti, N., Kusworo, T. D., Oktiawan, W., Wardhani, D. H. "Performance of Ultrafiltration-Ozone Combined Ssystem for Produced Water Treatment", Periodica Polytechnica Chemical Engineering, 63(3), pp. 438–447, 2019. https://doi.org/10.3311/PPch.13491

[13] Kusworo, T. D., Kumoro, A. C., Puspa, M. B., Citradhitya, P., Utomo, D. P. "Removal of ciprofloxacin-humic acid pollutant residue in wastewater through a hybrid treatment system consisting of pre-treatment with ozonation-AC/TiO_2/CeO_2 adsorption and degradation using PVDF/Ni-CeO_2@SiO_2 photocatalytic membrane", Journal of Environmental Chemical Engineering, 12(2), 112216, 2024. https://doi.org/10.1016/j.jece.2024.112216

[14] Pastrana-Martínez, L. M., Morales-Torres, S., Pérez-Molina, Á., Maldonado-Hódar, F. J. "Chapter 14 - Photocatalytic membranes: Synthesis, properties, and applications", In: Sakar, M., Balakrishna, R. G., Do, T.-O. (eds.) Photocatalytic Systems by Design: Materials, Mechanisms and Applications, Elsevier, 2021, pp. 385–406. ISBN 978-0-12-820532-7 https://doi.org/10.1016/B978-0-12-820532-7.00018-7

[15] Kusworo, T. D., Budiyono, Kumoro, A. C., Utomo, D. P. "Photocatalytic nanohybrid membranes for highly efficient wastewater treatment: A comprehensive review", Journal of Environmental Management, 317, 115357, 2022. https://doi.org/10.1016/j.jenvman.2022.115357

[16] Kusworo, T. D., Yulfarida, M., Kumoro, A. C., Utomo, D. P., Aryanti, N. "Effect of Nanophotocatalyst WO_3 Addition on PVDF Membrane Characteristics and Performance", Periodica Polytechnica Chemical Engineering, 68(3), pp. 338–347, 2024. https://doi.org/10.3311/PPch.24008

[17] Tabernero, A., González-Garcinuño, Á., Cardea, S., Marco, I. D., Martín del Valle, E. M. "PVDF-based membranes in biotechnology", Separation and Purification Technology, 365, 132636, 2025. https://doi.org/10.1016/j.seppur.2025.132636

[18] Liu, X., Liu, T., Ying, J., Yang, M., Zhang, Y., Tian, A. "Two dissociated viologen/anderson POM-based compounds for photocatalytic reduction of Cr(VI) under visible light", Journal of Molecular Structure, 1346, 143292, 2025. https://doi.org/10.1016/j.molstruc.2025.143292

[19] Kusworo, T. D., Wilukindra, Z. M., Atthoriq, M. A., Bella Puspa, M., Hanif, M. I., Puji Utomo, D. "Improvement of Effectiveness and Photocatalytic Properties of Poly(vinylidene Fluoride)-TiO_2-WO_3 Membrane with Polydopamine Modification for Natural Rubber Wastewater Treatment", Periodica Polytechnica Chemical Engineering, 69(3), pp. 385–402, 2025. https://doi.org/10.3311/PPch.40264

[20] Olajire, A. A. "Recent advances on the treatment technology of oil and gas produced water for sustainable energy industry-mechanistic aspects and process chemistry perspectives", Chemical Engineering Journal Advances, 4, 100049, 2020. https://doi.org/10.1016/j.ceja.2020.100049

[21] Hidup, Menteri Negara Lingkungan "Peraturan Menteri Negara Lingkungan Hidup Nomor 19 Tahun 2010 Tentang Baku Mutu Air Limbah Bagi Usaha dan/atau Kegiatan Minyak dan Gas Serta Panas Bumi" (Regulation of the State Minister for the Environment No. 19 of 2010 concerning Wastewater Quality Standards for Oil and Gas as well as Geothermal Business Activities), Jakarta, Indonesia, 2010. [online] Available at: https://jdih.kemenkoinfra.go.id/id/peraturan-menteri-negara-lingkungan-hidup-no-19-tahun-2010 [Accessed: 18 January 2026] (in Indonesian)

[22] SNI "SNI 06-6989.25-2005 Air dan air limbah – Bagian 25 : Cara uji kekeruhan dengan nefelometer" (SNI 06-6989.25-2005 Water and Wastewater -Part 25: Determination of Turbidity by Nephelometric Method), Standar Nasional Indonesia, Jakarta, Indonesia, 2005. (in Indonesian)

[23] SNI "SNI 6989.2:2019 Air dan air limbah – Bagian 2: Cara uji kebutuhan oksigen kimiawi (*chemical oxygen demand*/COD) dengan refluks tertutup secara spektrofotometri" (SNI 6989.2:2019 Water and Wastewater - Part 2: Determination of Chemical Oxygen Demand (COD) by Closed Reflux Spectrophotometric Method), Standar Nasional Indonesia, Jakarta, Indonesia, 2019. (in Indonesian)

[24] SNI "SNI 6989.72:2009 Air dan air limbah – Bagian 72: Cara uji Kebutuhan Oksigen Biokimia (*Biochemical Oxygen Demand*/BOD)" (SNI 6989.72:2009 Water and Wastewater Part 72: Determination of Biochemical Oxygen Demand (BOD)), Standar Nasional Indonesia, Jakarta, Indonesia, 2009. (in Indonesian)

[25] SNI "SNI 6989.10:2011 Air dan air limbah – Bagian 10: Cara uji minyak nabati dan minyak mineral secara gravimetri" (SNI 6989.10:2011 Water and Wastewater-Part 10: Determination of Vegetable Oil and Mineral Oil by Gravimetric Method), Standar Nasional Indonesia, Jakarta, Indonesia, 2009. (in Indonesian)

[26] SNI "SNI 06-6989.30-2005 Air dan air limbah – Bagian 30 : Cara uji kadar amonia dengan spektrofotometer secara fenat" (SNI 06-6989.30-2005 Water and waste water – Part 30: Test methods of ammonia content with spectrophotometers by phenates), Standar Nasional Indonesia, Jakarta, Indonesia, 2005. (in Indonesian)

[27] Ahmad, T., Rehman, L. M., Al-Nuaimi, R., de Levay, J.-P. B. B., Thankamony, R., Mubashir, M., Lai, Z. "Thermodynamics and kinetic analysis of membrane: Challenges and perspectives", Chemosphere, 337, 139430, 2023. https://doi.org/10.1016/j.chemosphere.2023.139430

[28] Taha, Y. R., Zrelli, A., Hajji, N., Alsalhy, Q., Shehab, M. A., Németh, Z., Hernadi, K. "Optimum content of incorporated nanomaterials: Characterizations and performance of mixed matrix membranes a review", Desalination and Water Treatment, 317, 100088, 2024. https://doi.org/10.1016/j.dwt.2024.100088

[29] Heinz, H., Pramanik, C., Heinz, O., Ding, Y., Mishra, R. K., …, Ziolo, R. F. "Nanoparticle decoration with surfactants: Molecular interactions, assembly, and applications", Surface Science Reports, 72(1), pp. 1–58, 2017. https://doi.org/10.1016/j.surfrep.2017.02.001

[30] Yi, Z., Zhu, L., Xiong, R., Fang, C., Zhu, B., Zhu, L., Zeng, H. "Advanced functional membranes based on amphiphilic copolymers", Progress in Polymer Science, 159, 101907, 2024. https://doi.org/10.1016/j.progpolymsci.2024.101907

[31] Han, Q., Wang, Y., Yang, Y., Han, Z., Li, S., Fang, J., Li, Y., Fang, P., Jin, B. "Multi-scale piezoelectric synergy: A porous $MoSe_2$/$BaTiO_3$@PVDF membrane for high-efficiency piezo-photocatalysis", Journal of Colloid and Interface Science, 702, 138994, 2026. https://doi.org/10.1016/j.jcis.2025.138994

[32] Martins, L. A., Pereira, N., Costa, C. M., Gomez-Tejedor, J. A., Lanceros-Mendez, S., Gomez Ribelles, J. L. "Increased electroactive properties of poly(vinylidene fluoride) films by thermo-mechanical post-processing", Surfaces and Interfaces, 75, 107814, 2025.
https://doi.org/10.1016/j.surfin.2025.107814

[33] Yeow, A. T. H., Chan, M. K., Ong, C. S., Ho, K. C. Effects of hydrogen bond donors on PVDF membrane modification using choline chloride-based deep eutectic solvents", Journal of Industrial and Engineering Chemistry, 139, pp. 514–524, 2024.
https://doi.org/10.1016/j.jiec.2024.05.028

[34] Kadir, E. S., Gayen, R. N. "Improved UV sensitivity in solution-processed PVDF/ZnO nanocomposites via piezo-phototronic effect", Materials Today Communications, 39, 109174, 2024.
https://doi.org/10.1016/j.mtcomm.2024.109174

[35] Veeralingam, S., Badhulika, S. "Low-density, stretchable, adhesive PVDF-polypyrrole reinforced gelatin based organohydrogel for UV photodetection, tactile and strain sensing applications", Materials Research Bulletin, 150, 111779, 2022.
https://doi.org/10.1016/j.materresbull.2022.111779

[36] Lu, T., Solis-Ramos, E., Yi, Y., Kumosa, M. "UV degradation model for polymers and polymer matrix composites", Polymer Degradation and Stability, 154, pp. 203–210, 2018.
https://doi.org/10.1016/j.polymdegradstab.2018.06.004

[37] Li, G., Zheng, W., Li, X., Luo, S., Xing, D., Ming, P., Li, B., Zhang, C. "Application of the Ce-based radical scavengers in proton exchange membrane fuel cells", International Journal of Hydrogen Energy, 74, pp. 17–30, 2024.
https://doi.org/10.1016/j.ijhydene.2024.05.393

[38] Kusworo, T. D., Soetrisnanto, D., Aryanti, N., Utomo, D. P., Qudratun, Tambunan, V. D., Simanjuntak, N. R. "Evaluation of Integrated modified nanohybrid polyethersulfone-ZnO membrane with single stage and double stage system for produced water treatment into clean water", Journal of Water Process Engineering, 23, pp. 239–249, 2018.
https://doi.org/10.1016/j.jwpe.2018.04.002

[39] Ratman, I., Kusworo, T. D., Utomo, D. P., Azizah, D. A., Ayodyasena, W. A. "Petroleum Refinery Wastewater Treatment using Three Steps Modified Nanohybrid Membrane Coupled with Ozonation as Integrated Pre-treatment", Journal of Environmental Chemical Engineering, 8(4), 103978, 2020.
https://doi.org/10.1016/j.jece.2020.103978

[40] Rekhate, C. V., Srivastava, J. K. "Recent advances in ozone-based advanced oxidation processes for treatment of wastewater-A review", Chemical Engineering Journal Advances, 3, 100031, 2020.
https://doi.org/10.1016/j.ceja.2020.100031

[41] Cséfalvay, E., Nöthe, T., Mizsey, P. "Modelling of wastewater ozonation - Determination of reaction kinetic constants and effect of temperature", Periodica Polytechnica Chemical Engineering, 51(2), pp. 13–17, 2007.
https://doi.org/10.3311/pp.ch.2007-2.03

[42] Manasfi, T. "Chapter Four - Ozonation in drinking water treatment: an overview of general and practical aspects, mechanisms, kinetics, and byproduct formation", In: Manasfi, T., Boudenne, J.-L. (eds.) Comprehensive Analytical Chemistry, Elsevier, 2021, pp. 85–116. ISBN 978-0-444-64343-8
https://doi.org/10.1016/bs.coac.2021.02.003

[43] Bahmanzadegan, F., Ghaemi, A. "A comprehensive review on novel zeolite-based adsorbents for environmental pollutant", Journal of Hazardous Materials Advances, 17, 100617, 2025.
https://doi.org/10.1016/j.hazadv.2025.100617

[44] Li, S., Ni, G., Wang, H., Xun, M., Xu, Y. "Effects of acid solution of different components on the pore structure and mechanical properties of coal", Advanced Powder Technology, 31(4), pp. 1736–1747, 2020.
https://doi.org/10.1016/j.apt.2020.02.009

[45] Shen, J., Yuan, Y., Duan, F., Li, Y. "Performance of resin adsorption and ozonation pretreatment in mitigating organic fouling of reverse osmosis membrane", Journal of Water Process Engineering, 53, 103688, 2023.
https://doi.org/10.1016/j.jwpe.2023.103688